Rhodium(III) and Iridium(III) Solvates of the Form $[(\eta^5\text{-}C_5Me_5)M(S)_3]^{2+}$ as Models for the Reactivity of Half-Sandwich Compounds[1]

Antonio Cusanelli, Lynda Nicula-Dadci, Urban Frey, and André E. Merbach*

Institut de Chimie Minérale et Analytique, Université de Lausanne, CH-1015 Lausanne, Switzerland

Received November 18, 1996[⊗]

Solvent exchange on the half-sandwich organic solvates $[(\eta^5\text{-}C_5Me_5)M(S)_3]^{2+}$ (M = Rh, S = MeCN **(1)** or Me_2SO **(3)**; and M = Ir, S = MeCN **(2)** or Me_2SO **(4)**) has been investigated as a function of temperature, pressure, and concentration of free solvent by ^1H NMR line-broadening techniques in CD_3CN and/or CD_3NO_2. The exchange rates span several orders of magnitude, from $k_{ex}^{298} = 8.8 \times 10^{-2}$ s^{-1} for **2** to 3.6×10^3 s^{-1} for **3**, as a result of changes in the electronic and steric properties of the ligands. Nevertheless, the volume of activation remains consistently positive for compounds **1**−**4** with values ranging from +0.8 to +3.3 cm^3 mol^{-1}. In combination with the positive activation entropies obtained and the first-order rate law established for these systems, it was concluded that regardless of the nature of the ligand the solvent exchange process on **1**−**4** proceeds *via* a dissociative D mechanism. Of note, the intermolecular exchange with free Me_2SO on **4** takes place exclusively from a conformational isomer of **4** (structure **4.2**), which is itself in equilibrium with a second, more compact conformer (structure **4.1**).

Introduction

The rate of solvent exchange (eq 1), as characterized by the rate constant, k_{ex}, can be taken as a measure of the "lability" of the solvated metal ion $[MS_n]^{q+}$. The values obtained for k_{ex}

$$[MS_n]^{q+} + n^*S \overset{k_{ex}}{\rightleftharpoons} [M^*S_n]^{q+} + nS \qquad (1)$$

are thus of fundamental significance, and considerable effort has been made over the years to determine k_{ex} for a wide variety of metals and solvents and, in turn, to elucidate the respective mechanism of solvent exchange. Accordingly, recent quantitative kinetic studies on the hexaaqua compounds of rhodium(III) and iridium(III), conducted in our laboratory, led to extremely slow water exchange rate constants of 2.2×10^{-9} and 1.1×10^{-10} s^{-1}, respectively.[3] In both cases, the parameters obtained were supportive of an associative interchange mechanism. Interestingly, substitution of three ligated water molecules in these compounds by a η^5-C_5Me_5 moiety (i.e., $[(\eta^5\text{-}C_5Me_5)M(H_2O)_3]^{2+}$ where M = Rh or Ir) resulted in a dramatic increase of 14 orders of magnitude in the respective water exchange rate constants and, more importantly, this increase was also accompanied by a changeover in mechanism.[4] The kinetic data obtained for these half-sandwich compounds, although preliminary, were suggestive of an interchange mechanism. Therefore, to clarify the mechanism responsible for solvent exchange on these half-sandwich species and to possibly provide further insight into the kinetic behavior observed for the $[M(H_2O)_6]^{3+}$/$[(\eta^5\text{-}C_5Me_5)M(H_2O)_3]^{2+}$ couples, we have extended our kinetic investigation to other specific half-sandwich solvento compounds. In this paper we report the results of a variable temperature, variable pressure, and variable ligand concentration ^1H NMR study on $[(\eta^5\text{-}C_5Me_5)M(S)_3]^{2+}$ (M = Rh, S = MeCN (**1**) or Me_2SO (**3**); and M = Ir; S = MeCN **(2)** or Me_2SO (**4)**). A rate law for the exchange process is established, and a discussion of the mechanism of solvent exchange for **1**−**4** and the half-sandwich aqua analogs is provided.

Experimental Section

General Methods and Syntheses. All manipulations were performed under argon by using standard Schlenk or vacuum line techniques unless stated otherwise. $AgPF_6$ (Aldrich), $[(\eta^5\text{-}C_5Me_5)RhCl_2]_2$ (Aldrich), $[(\eta^5\text{-}C_5Me_5)IrCl_2]_2$ (Aldrich), and Celatom FW-50 filter agent (Aldrich) were used as received. Dimethyl sulfoxide (Me_2SO, Fluka) was dried over 3-Å molecular sieves for 48 h and used immediately thereafter. Acetonitrile (MeCN, Fluka) was distilled from calcium hydride, diethyl ether (Et_2O, Fluka) from sodium benzophenone ketyl, and acetone (Me_2CO, Fluka) from calcium sulfate; all were distilled under nitrogen and used immediately. $[(\eta^5\text{-}C_5Me_5)M(S)_3](PF_6)_2$ (M = Rh, S = MeCN (**1**) or Me_2SO (**3**); and M = Ir; S = MeCN (**2**) or Me_2SO (**4)**) were prepared by modification to the literature method.[5]

Preparation of $[(\eta^5\text{-}C_5Me_5)Rh(MeCN)_3](PF_6)_2$ (1). This compound was prepared from $[(\eta^5\text{-}C_5Me_5)RhCl_2]_2$ (0.80 g, 1.30 mmol) and silver hexafluorophosphate (1.30 g, 5.20 mmol) with acetonitrile as the coordinating solvent. The product was recrystallized from acetonitrile/diethyl ether and subsequently dried *in vacuo* to give **1** as a yellow-orange solid in 33% yield (0.55 g, 0.85 mmol). ^1H NMR (CD_3NO_2, 270.0 K): δ 1.85 (s, 15H, η^5-C_5Me_5), 2.50 (s, 9H, MeCN). Anal. Calcd: C, 29.51; H, 3.71; N, 6.45; F, 35.01. Found: C, 29.36; H, 3.64; N, 6.32; F, 34.86.

Preparation of $[(\eta^5\text{-}C_5Me_5)Ir(MeCN)_3](PF_6)_2$ (2). This compound was prepared in a manner analogous to that of compound **1** using $[(\eta^5\text{-}C_5Me_5)IrCl_2]_2$ (0.80 g, 1.00 mmol) and silver hexafluorophosphate (1.00 g, 4.00 mmol). After recrystallization from acetonitrile/diethyl ether, compound **2** was obtained as a yellow solid in 49% yield (0.72 g, 0.97 mmol). ^1H NMR (CD_3NO_2, 319.9 K): δ 1.85 (s, 15H, η^5-C_5Me_5), 2.68 (s, 9H, MeCN). Anal. Calcd: C, 25.95; H, 3.27; N, 5.67; F, 30.79. Found: C, 26.02; H, 3.38; N, 5.59; F, 30.70.

Preparation of $[(\eta^5\text{-}C_5Me_5)Rh(Me_2SO)_3](PF_6)_2$ (3). $[(\eta^5\text{-}C_5Me_5)RhCl_2]_2$ (0.80 g, 1.30 mmol) was taken up in dimethyl sulfoxide (10 mL), and silver hexafluorophosphate (1.30 g, 5.20 mmol) was then quickly added to the stirring mixture. Silver chloride was then removed

[⊗] Abstract published in *Advance ACS Abstracts,* April 15, 1997.

(1) High Pressure NMR Kinetics. 75. Part 74: See ref 2.
(2) Powell, D. H.; Ni Dhubhghaill, O. M.; Pubanz, D.; Helm, L.; Lebedev, Y. S.; Schlaepfer, W.; Merbach, A. E. *J. Am. Chem. Soc.* **1996**, *118*, 9333.
(3) Cusanelli, A.; Frey, U.; Richens, D. T.; Merbach, A. E. *J. Am. Chem. Soc.* **1996**, *118*, 5265.
(4) Dadci, L.; Elias, H.; Frey, U.; Hörnig, A.; Koelle, U.; Merbach, A. E.; Paulus, H.; Schneider, J. S. *Inorg. Chem.* **1995**, *34*, 306.
(5) White, C.; Thompson, S. J.; Maitlis, P. M. *J. Chem. Soc., Dalton Trans.* **1977**, 1654.

S0020-1669(96)01380-8 CCC: $14.00

by centrifugation in air, and the remaining orange supernatant solution was then filtered through a short column of Celatom FW-50. The solution was then added to rapidly stirring diethyl ether (200 mL) in a dropwise fashion, the diethyl ether was decanted off, and the remaining orange solid was then dried *in vacuo* for several hours. Recrystallization from a minimum volume of acetone, a few drops of dimethyl sulfoxide, and diethyl ether and subsequent drying *in vacuo* gave **3** as an orange solid in 28% yield (0.55 g, 0.73 mmol). IR (acetone): 933 cm^{-1} ν(SO). ^1H NMR (CD_3NO_2, 232.4 K): δ 1.67 (s, 15H, η^5-C_5Me_5), 2.92 (s, 18H, Me_2SO). Anal. Calcd: C, 25.20; H, 4.36; S, 12.62; F, 29.90. Found: C, 25.18; H, 4.27; S, 12.40; F, 29.72.

Preparation of $[(\eta^5\text{-}C_5Me_5)Ir(Me_2SO)_3](PF_6)_2$ (4). This compound was prepared by the procedure described previously for compound **3** using $[(\eta^5\text{-}C_5Me_5)IrCl_2]_2$ (0.80 g, 1.00 mmol) and silver hexafluorophosphate (1.00 g, 4.00 mmol). After recrystallization from acetone/dimethyl sulfoxide/diethyl ether, compound **4** was obtained as a yellow solid in 26% yield (0.44 g, 0.52 mmol). IR (acetone): 1126 cm^{-1} ν(SO). ^1H NMR (CD_3NO_2, 243.2 K): δ 1.64 (s, 15H, η^5-C_5Me_5; **4.2**), 1.79 (s, 15H, η^5-C_5Me_5; **4.1**), 2.99 (s, 18H, Me_2SO; **4.2**), 3.11 (s, 6H, Me_2SO; **4.1**), 3.15 (s, 6H, Me_2SO; **4.1**), 3.16 (s, 6H, Me_2SO; **4.1**). $^{13}C\{^1H\}$ NMR (CD_3NO_2, 243.2 K): δ 8.92 (s, η^5-$C_5\mathit{Me}_5$; **4.2**), 9.56 (s, η^5-$C_5\mathit{Me}_5$; **4.1**), 39.33 (s, Me_2SO; **4.2**), 39.55 (s, Me_2SO; **4.1**), 40.36 (s, Me_2SO; **4.1**), 41.59 (s, Me_2SO; **4.1**), 85.40 (s, η^5-C_5Me_5; **4.2**), 94.10 (s, η^5-C_5Me_5; **4.1**). Anal. Calcd: C, 22.56; H, 3.91; S, 11.29; F, 26.77. Found: C, 22.70; H, 3.84; S, 11.12; F, 26.51.

IR and Variable Temperature NMR Measurements. Infrared spectra of solutions in NaCl cells were obtained by using a Perkin-Elmer 1600 Series FT-IR instrument. All NMR spectra were recorded on a Bruker ARX 400 instrument at operating frequencies of 400 and 100 MHz for ^1H and ^{13}C nuclei, respectively. ^1H NMR was used for characterization and kinetic work whereas $^{13}C\{^1H\}$ NMR was utilized solely for characterization. A standard Bruker program was used to acquire the 2D ^1H NMR EXCSY spectrum. CD_3NO_2 (Armar, 99.5 atom % D) and CD_3CN (Armar, 99.8 atom % D) were dried over 3-Å molecular sieves and CaH_2, respectively. CD_3NO_2 was used both as a solvent and as an internal field lock for the variable concentration measurements on compounds **1** and **2** and for all the NMR work on compounds **3** and **4**. CH_3CN/CD_3CN (95:5) was used for the variable temperature and pressure measurements on **1** and **2**. All of the NMR solutions were prepared under an inert atmosphere by weighing, and the concentrations are given in molality (mol kg^{-1} of solvent). A 1−3% concentration of tetramethylsilane (TMS) (Armar) was added as a shift and field homogeneity reference. Plots of chemical shift vs temperature in the slow exchange region were determined for bound Me_2SO in compounds **3** and **4**, and the results were then incorporated into the line shape analysis; no chemical shift dependence on temperature was observed for compounds **1** and **2**. Ordinary 5 mm tubes were employed for the variable temperature measurements on **1**, **3**, and **4**, but a 5 mm sapphire tube[3] was used for the same measurements on **2** because of the high temperatures (above the boiling point of the solvent at ambient pressure) required. The temperature was controlled to within ±0.2 K using a Bruker B-VT 2000 instrument and was measured before and after spectral acquisition by substitution of the NMR tube for a platinum resistor.[6]

Variable Pressure NMR Measurements. The variable pressure NMR spectra were measured using a newly designed high-resolution, high-pressure probe. This probe was constructed for a narrow-bore (50 mm ∅) NMR cryomagnet, and a schematic drawing illustrating the central component of the probe is shown in Figure 1. The upper and lower components (both not shown) contain the liquid and the electronic connections, respectively. The high-pressure vessel (Figure 1) is made of nonmagnetic beryllium−copper alloy, Berylco-25, with an outer diameter of 27 mm, an inner diameter of 17 mm, and an inner length of 170 mm. The vessel has a calculated bursting pressure of 560 MPa and has been tested up to 240 MPa. The probe is generally used for pressures ranging from 0.1 to 200 MPa. A double helix was cut into the outside of the vessel for the circulation of the thermostating liquid and can thus accommodate a temperature range between 230 and 420 K. The temperature gradient over the sample region was found to be less than ±0.3 K, and the temperature stability is better than ±0.2 K over the whole pressure range. For temperatures above 320 K, thermal insulation against the shim coil unit is obtained by circulating water through the double helix cut into the aluminum support. In the bottom of the Berylco vessel is located a platinum 100 Ω resistor for temperature measurements.

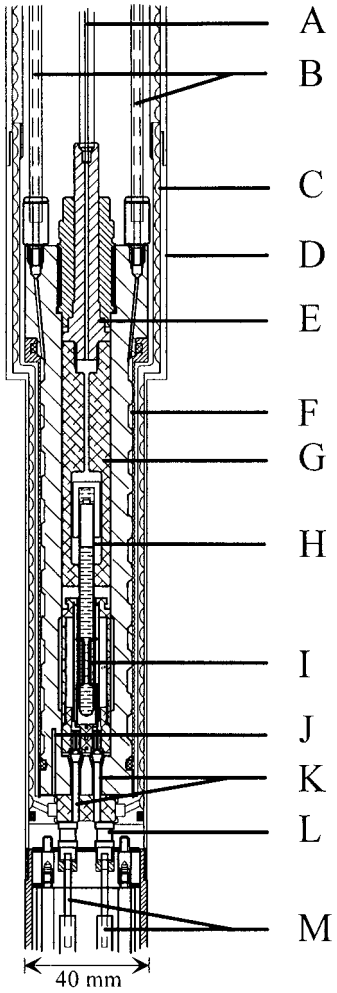

Figure 1. Schematic drawing of the high-pressure, high-resolution ^1H NMR (400 MHz) probe for a narrow-bore cryomagnet: (A) pressurizing fluid inlet; (B) thermostatization inlet and outlet; (C) thermal insulation by water circulation; (D) aluminum support; (E) Berylco plug; (F) double helix for themostatization; (G) sample holder; (H) 5 mm o.d. NMR tube with Macor seal; (I) NMR coil; (J) Pt 100 Ω resistor; (K) RF leadthrough; (L) matching/tuning capacitors; and (M) screwdrivers for matching/tuning.

The internal Vespel component, the sample holder, and the support containing the saddle-shaped coil made by Spectrospin (Fällanden, Switzerland) are also shown in Figure 1. An electronic circuit was built for ^1H (400 MHz) observation and ^2H (61.4 MHz) field lock, and the frequencies can be adjusted from outside the magnet. The following characteristics were obtained for this probe for when it is used for ^1H NMR measurements. On a sample containing 10% $CHCl_3$ in acetone-d_6, we obtain a nonspinning resolution of 0.4 Hz and a line width at the ^{13}C satellite level of 30 Hz. This relatively poor line shape compared to that obtained for commercial ambient pressure probes, caused mainly by the presence of the pressurizing liquid around the NMR coil, significantly decreases the sensitivity of the probe. Using the standard sample for sensitivity tests (0.1% ethylbenzene in $CDCl_3$) and applying a 90° pulse length of 17 μs, we obtain a signal to noise ratio of 70:1 compared with 330:1 for a Bruker 5 mm ^1H NMR probe also working at 400 MHz. A resolution of approximately 1 Hz is obtained for routine work. The high-pressure NMR sample tube and the experimental setup were described previously.[7]

(6) Ammann, C.; Meier, P.; Merbach, A. E. *J. Magn. Reson.* **1982**, *46*, 319.

Table 1. Effect of Temperature on the Rate Constant, k_{ex}, for MeCN Exchange on the Acetonitrile Compounds[a]

$[(\eta^5\text{-}C_5Me_5)Rh(MeCN)_3](PF_6)_2$ (**1**)[b]		$[(\eta^5\text{-}C_5Me_5)Ir(MeCN)_3](PF_6)_2$ (**2**)[c]	
T (K)	k_{ex} (s^{-1})	T (K)	k_{ex} (s^{-1})
280.4	5.0	340.7	7.2
286.5	9.8	343.2	9.3
291.6	18.7	345.8	12.9
297.4	34	351.7	20.5[d]
299.9	43	353.9	24[d]
301.9	66	359.9	39[d]
302.2	55	370.6	100[d]
305.6	76		
308.9	114		

[a] In CH_3CN/CD_3CN (95:5). [b] [Compound] = 0.116 m; ambient pressure. [c] [Compound] = 0.107 m; ambient pressure. [d] Values determined using a sapphire NMR tube.

Computational Methods. The rate constants reported were obtained from line-broadened spectra, and their analysis using the required equations was accomplished by a nonlinear least-squares program fitting the desired parameter values. Reported errors are 1 standard deviation.

Results

(i) Kinetic Measurements on the Acetonitrile Compounds. At 258.6 K, the ^{1}H NMR spectrum of $[(\eta^5\text{-}C_5Me_5)Rh(MeCN)_3](PF_6)_2$ **(1)** in CH_3CN/CD_3CN (95:5) exhibited two resonances at 2.42 and 1.99 ppm corresponding to bound and free MeCN, respectively; the signal of bound acetonitrile is narrow and well separated from that of free acetonitrile. As the temperature was raised to 308.9 K, the bound signal began to broaden, indicating that an intermolecular exchange with free solvent was occurring (eq 2). Similar kinetic behavior was found for the iridium

$$[(\eta^5\text{-}C_5Me_5)M(MeCN)_3]^{2+} + 3{*}MeCN \overset{k_{ex}}{\rightleftharpoons} [(\eta^5\text{-}C_5Me_5)M(*MeCN)_3]^{2+} + 3MeCN \quad (2)$$

(M = Rh or Ir)

analog $[(\eta^5\text{-}C_5Me_5)Ir(MeCN)_3](PF_6)_2$ **(2)**; the ^{1}H NMR spectrum of **2** showed two resonances at 324.2 K, and elevating the temperature also resulted in a broadening of the bound resonance (eq 2). From a least-squares fit of the bound resonance to a Lorentzian curve, the transverse relaxation rate of the acetonitrile protons, $1/T_2^b$ (s^{-1}), and in the limit of slow exchange[8] the rate constant, k_{ex}, for the solvent exchange process (after corrections for inhomogeneity, $1/T_2{*}$) were determined for **1** and **2** ($k_{ex} = 1/T_2^b - 1/T_2{*}$).

The variable temperature rate constants (Table 1), measured between 280.4 and 308.9 K for compound **1** and between 340.7 and 370.6 K for compound **2**, were least-squares fitted using the Eyring equation (eq 3) to give the rate constants and activation parameters presented in Table 2. The pressure

$$k_{ex} = (k_B T/h) \exp[(\Delta S^{\ddagger}/R) - (\Delta H^{\ddagger}/RT)] \quad (3)$$

dependence of the rate constants for **1** and **2** (Table 3) was measured at 301.3 and 360.7 K, respectively, and subsequently these data were least-squares fitted using eq 4 to give the activation parameters summarized in Table 2.

$$\ln k_{ex} = \ln k_{ex0} - \Delta V^{\ddagger} P/RT \quad (4)$$

For compounds **1** and **2**, the free acetonitrile concentration dependence of the exchange rate constant, k_{ex}, was investigated in the inert diluent CD_3NO_2. The experimental spectra and the rate constants obtained from least-squares fitting of the spectra using the Kubo−Sack method[9] for both **1** and **2** (Figure 2) infer that k_{ex} is independent of the concentration of free solvent.

(ii) Kinetic Measurements on the Dimethyl Sulfoxide Compounds. As was observed for the acetonitrile compounds **1** and **2**, the ^{1}H NMR spectrum of the rhodium dimethyl sulfoxide compound $[(\eta^5\text{-}C_5Me_5)Rh(Me_2SO)_3](PF_6)_2$ **(3)**, recorded at 232.4 K in CD_3NO_2 containing excess free Me_2SO, exhibited two resonances at 2.92 and 2.56 ppm, assigned to bound and free Me_2SO, respectively (Figure 3). These signals began to broaden as the temperature was elevated, eventually giving rise to an averaged signal at 302.6 K. This behavior is consistent with an intermolecular exchange with free solvent (eq 5).

$$[(\eta^5\text{-}C_5Me_5)Rh(Me_2SO)_3]^{2+} + 3{*}Me_2SO \overset{k_{ex}}{\rightleftharpoons} [(\eta^5\text{-}C_5Me_5)Rh(*Me_2SO)_3]^{2+} + 3Me_2SO \quad (5)$$

In stark contrast to compounds **1**, **2**, and its rhodium analog **3**, the low-temperature ^{1}H NMR spectrum of $[(\eta^5\text{-}C_5Me_5)Ir(Me_2SO)_3](PF_6)_2$ **(4)**, acquired at 243.2 K in CD_3NO_2 containing excess free Me_2SO, did not show the expected two resonances corresponding to bound and free Me_2SO, but instead exhibited *five* resonances at 3.16, 3.15, 3.11, 2.99, and 2.56 ppm (Figure 3); the latter was unequivocally assigned to free solvent, and the remaining signals were attributed to **4**. Also present in this spectrum were two unequally populated resonances at 1.79 and 1.64 ppm, assigned to two unique $\eta^5\text{-}C_5Me_5$ groups.[10] The three resonances at 3.16−3.11 ppm integrated to 6 protons each with respect to the more populated of the $\eta^5\text{-}C_5Me_5$ signals whereas the remaining bound Me_2SO resonance at 2.99 ppm integrated to 18 protons with respect to the less populated $\eta^5\text{-}C_5Me_5$ moiety. Taken together, these results clearly suggest the presence of two stereoisomers of **4** (denoted as major and minor in Figure 3), each composed of a $\eta^5\text{-}C_5Me_5$ group and three Me_2SO ligands.

As the temperature was raised to 314.2 K, all five resonances began to broaden, indicating that an intramolecular process and/or an intermolecular exchange(s) with free solvent was occurring over the same temperature interval (Figure 3). Similar spectra were obtained when the variable temperature study was repeated without excess Me_2SO, thus corroborating the interconversion between the two isomers of **4**. Notably, $^{13}C\{^1H\}$ NMR spectra of **4**, in the absence of free Me_2SO, acquired over a similar temperature interval provided further evidence in support of an interconversion process; at 243.2 K three signals due to the major isomer of **4** and one resonance due to the minor isomer of **4** were observed whereas at 289.2 K a single broad resonance was found. A 2D ^{1}H NMR EXCSY (exchange correlation spectroscopy) spectrum of **4** in CD_3NO_2 at 243.5 K with excess Me_2SO exhibited an intense cross peak for the minor isomer/free Me_2SO couple and smaller cross peaks for the minor isomer/major isomer couples.[10] Most importantly, the cross peaks diagnostic of an intermolecular exchange between the major isomer and free Me_2SO were not observed, thus indicating that (i) the interconversion between the major and minor isomers of **4** proceeds by an intramolecular pathway (eq 6) and (ii) the exchange with free Me_2SO proceeds solely from the minor conformer (eq 7).

(7) Frey, U.; Helm, L.; Merbach, A. E. *High Pressure Res.* **1990**, *2*, 237.
(8) McLaughlin, A. C.; Leigh, J. S. *J. Magn. Reson.* **1973**, *9*, 296.
(9) Delpuech, J. J.; Ducom, J.; Michon, V. *Bull. Soc. Chim. Fr.* **1971**, 1848.
(10) Cusanelli, A.; Frey, U; Merbach, A. E. *J. Chem. Soc., Chem. Commun.* **1997**, 379.

Table 2. Rate Constants and Activation Parameters for Solvent Exchange on Rhodium(III) and Iridium(III) Solvates[a,b]

solvate	k_{ex}^{298} (s^{-1})	$\Delta H^{\ddagger}$ (kJ mol^{-1})	$\Delta S^{\ddagger}$ (J mol^{-1} K^{-1})	$\Delta V^{\ddagger}$ (cm^3 mol^{-1})	mech
$[Rh(H_2O)_6]^{3+}$ [c]	$(2.2 \pm 2.7) \times 10^{-9}$	131 ± 23	$+29 \pm 69$	-4.2 ± 0.6	I_a
$[Ir(H_2O)_6]^{3+}$ [c]	$(1.1 \pm 0.1) \times 10^{-10}$	130.5 ± 0.6	$+2.1 \pm 1.7$	-5.7 ± 0.5	I_a
$[(\eta^5\text{-}C_5Me_5)Rh(H_2O)_3]^{2+}$ [d]	$(1.6 \pm 0.3) \times 10^{5}$	65.6 ± 7.0	$+75 \pm 24$	$+0.6 \pm 0.6$	D
$[(\eta^5\text{-}C_5Me_5)Ir(H_2O)_3]^{2+}$ [d]	$(2.5 \pm 0.1) \times 10^{4}$	54.9 ± 3.0	$+24 \pm 8$	$+2.4 \pm 0.5$	D
$[(\eta^5\text{-}C_5Me_5)Rh(MeCN)_3]^{2+}$ (**1**)[e]	$(3.7 \pm 0.1) \times 10^{1}$	76.7 ± 1.8	$+42 \pm 6$	$+0.8 \pm 0.5$	D
$[(\eta^5\text{-}C_5Me_5)Ir(MeCN)_3]^{2+}$ (**2**)[e]	$(8.8 \pm 0.9) \times 10^{-2}$	85.9 ± 2.6	$+23 \pm 7$	$+1.5 \pm 0.8$	D
$[(\eta^5\text{-}C_5Me_5)Rh(Me_2SO)_3]^{2+}$ (**3**)[f]	$(3.6 \pm 0.1) \times 10^{3}$	54.6 ± 0.3	$+6.4 \pm 1.1$	$+3.3 \pm 0.1$	D
$[(\eta^5\text{-}C_5Me_5)Ir(Me_2SO)_3]^{2+}$ (**4**)[g]	$(2.5 \pm 0.1) \times 10^{3}$	60.3 ± 1.4	$+22 \pm 5$	$+2.8 \pm 0.4$	D

[a] All values refer to the exchange of one particular solvent molecule. [b] Kinetic parameters associated with the intramolecular isomerization process on **4**: $k_{intra}^{298} = (7.9 \pm 0.4) \times 10^2$ s^{-1}; $\Delta H^{\ddagger} = 66.7 \pm 1.6$ kJ mol^{-1}; $\Delta S^{\ddagger} = +34 \pm 6$ J mol^{-1} K^{-1}; $\Delta V_{intra}^{\ddagger} = +9.2 \pm 0.5$ cm^3 mol^{-1}. [c] See ref 3. [d] See ref 4. [e] In CH_3CN/CD_3CN (95:5). [f] O-Bonded exchange in CD_3NO_2 diluent. [g] S-Bonded exchange in CD_3NO_2 diluent.

Table 3. Effect of Pressure on the Rate Constant, k_{ex}, for MeCN Exchange on the Acetonitrile Compounds[a]

$[(\eta^5\text{-}C_5Me_5)Rh(MeCN)_3](PF_6)_2$ (**1**)[b]		$[(\eta^5\text{-}C_5Me_5)Ir(MeCN)_3](PF_6)_2$ (**2**)[c]	
P (MPa)	k_{ex} (s^{-1})	P (MPa)	k_{ex} (s^{-1})
0.1	71	3.6	58
0.1	67	3.2	65
28.1	71	25.9	55
50.7	71	50.7	52
79.2	72	76.8	53
102.0	75	100.7	53
128.2	68	129.2	55
148.2	70	149.3	55
174.8	68	178.0	53
195.4	67	199.4	54

[a] In CH_3CN/CD_3CN (95:5). [b] [Compound] = 0.116 m at 301.3 K. [c] [Compound] = 0.107 m at 360.7 K.

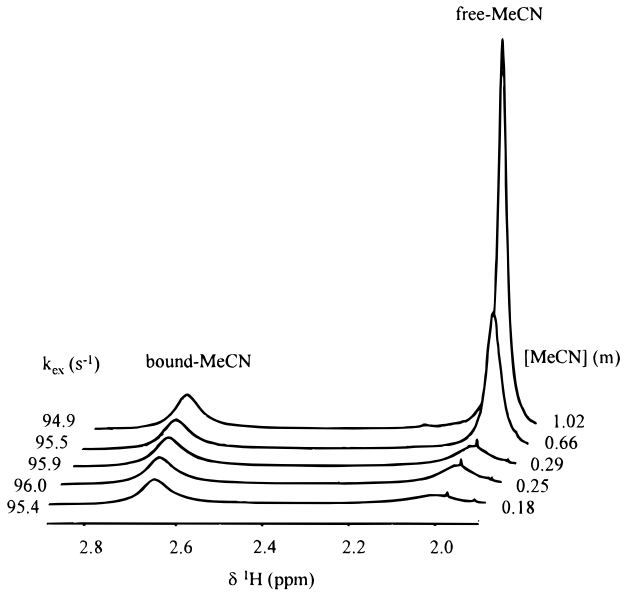

Figure 2. Experimental ^{1}H NMR (400 MHz) spectra of $[(\eta^5\text{-}C_5Me_5)Ir(MeCN)_3](PF_6)_2$ **(2)** (0.096 m) in CD_3NO_2 diluent with various concentrations of MeCN at 372.7 K.

$$\text{major-}[(\eta^5\text{-}C_5Me_5)Ir(Me_2SO)_3]^{2+} \overset{k_{intra}}{\rightleftharpoons} \text{minor-}[(\eta^5\text{-}C_5Me_5)Ir(Me_2SO)_3]^{2+} \quad (6)$$

$$\text{minor-}[(\eta^5\text{-}C_5Me_5)Ir(Me_2SO)_3]^{2+} + 3{*}Me_2SO \overset{k_{ex}}{\rightleftharpoons} \text{minor-}[(\eta^5\text{-}C_5Me_5)Ir(*Me_2SO)_3]^{2+} + 3Me_2SO \quad (7)$$

The rate constant, k_{ex}, for the solvent exchange process on **3** (eq 5) was determined from a simple Kubo−Sack two-site exchange matrix using the line shape analysis program ECHANGE.[11] However, on the basis of the 2D ^{1}H NMR results, a more complex Kubo−Sack five-site matrix for the

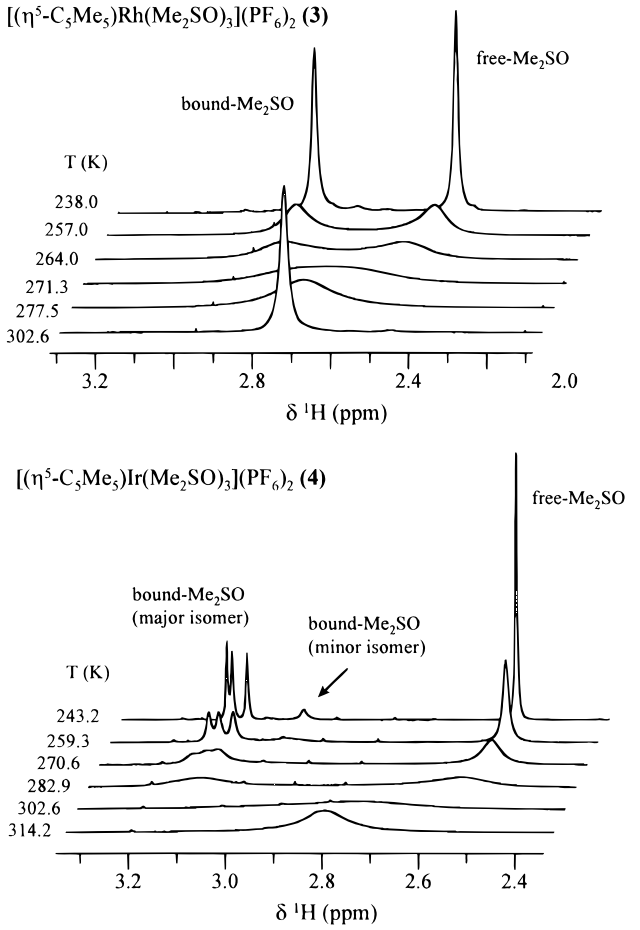

Figure 3. Experimental ^{1}H NMR (400 MHz) spectra of $[(\eta^5\text{-}C_5Me_5)Rh(Me_2SO)_3](PF_6)_2$ **(3)** (0.100 m in compound; [free Me_2SO] = 0.304 m) and $[(\eta^5\text{-}C_5Me_5)Ir(Me_2SO)_3](PF_6)_2$ **(4)** (0.010 m in compound; [free Me_2SO] = 0.028 m) in CD_3NO_2 diluent at various temperatures and ambient pressure.

bound Me_2SO and free Me_2SO resonances was constructed for compound **4** and was used for line shape analysis to obtain the rate constants both for the intramolecular interconversion process, k_{intra}, and for the intermolecular solvent exchange, k_{ex} (eqs 6 and 7). The intramolecular rate constants obtained for **4** from line shape analysis of the bound Me_2SO resonances in the presence and in the absence of free Me_2SO were similar and thus confirmed that k_{intra} was independent of the concentration of free Me_2SO. Similar values for k_{intra} were also obtained from line shape fittings of the $\eta^5\text{-}C_5Me_5$ resonances.

The variable temperature rate constants for **3** and **4** (Table 4) were least-squares fitted using eq 3, leading to the rate constants and activation parameters presented in Table 2. The

(11) ECHANGE derived from EXCNG (see ref 9).

Table 4. Effect of Temperature on the Rate Constants k_{intra} and k_{ex}, and on the Equilibrium Constant K_{eq} for Me_2SO Exchange on the Dimethyl Sulfoxide Compounds[a]

$[(\eta^5\text{-}C_5Me_5)Rh(Me_2SO)_3](PF_6)_2$ (**3**)[b]		$[(\eta^5\text{-}C_5Me_5)Ir(Me_2SO)_3](PF_6)_2$ (**4**)[c]			
T (K)	k_{ex} (s^{-1})	T (K)	k_{ex} (s^{-1})	k_{intra} (s^{-1})	K_{eq}[d]
238.0	10.7	243.2			0.17
244.9	25.3	248.3			0.20
251.0	49	253.4			0.23
257.0	95	259.3	62	11.9	0.28
260.6	133	264.8	109	23.3	0.32
264.0	185	270.6	185	45	(0.38)
267.3	257	276.6	327	92	(0.44)
269.1	297	282.9	552	200	(0.52)
271.3	370	289.2	1040	332	(0.59)
275.1	512	302.6	3750	971	(0.80)
277.5	634	314.2	9960	3610	(1.01)
289.3	1730				
302.6	5340				

[a] In CD_3NO_2 diluent. [b] O-Bonded exchange; [compound] = 0.100 m; [Me_2SO] = 0.304 m; ambient pressure. [c] S-Bonded exchange; [compound] = 0.010 m; [Me_2SO] = 0.028 m; ambient pressure. [d] K_{eq} = [minor isomer]/[major isomer]; $K_{eq}^{298} = 0.74 \pm 0.03$; values in parentheses were calculated from $\Delta H°$ and $\Delta S°$ whereas the nonparenthesized values were determined experimentally.

Table 5. Effect of Pressure on the Rate Constants k_{intra}, k_{ex}, and on the Equilibrium Constant K_{eq} for Me_2SO Exchange on the Dimethyl Sulfoxide Compounds[a]

$[(\eta^5\text{-}C_5Me_5)Rh(Me_2SO)_3](PF_6)_2$ (**3**)[b]		$[(\eta^5\text{-}C_5Me_5)Ir(Me_2SO)_3](PF_6)_2$ (**4**)[c]			
P (MPa)	k_{ex} (s^{-1})	P (MPa)	k_{ex} (s^{-1})	k_{intra} (s^{-1})	K_{eq}[d]
0.1	522	0.1	113	25.1	0.40
0.1	521	0.1	117	25.8	0.42
25.0	500	26.5	112	23.0	0.37
49.1	484	48.2	105	19.9	0.32
75.5	464	74.6	101	18.0	0.28
100.8	446	100.5	100	15.8	0.24
124.4	434	124.5	104	14.0	0.21
149.0	417	148.0	95	13.1	0.20
164.1	410	172.2	96	11.8	0.18
180.2	403	197.8	84	11.9	0.19

[a] In CD_3NO_2 diluent. [b] O-Bonded exchange; [compound] = 0.100 m; [Me_2SO] = 0.304 m; temperature = 276.0 K. [c] S-Bonded exchange; [compound] = 0.010 m; [Me_2SO] = 0.026 m; temperature = 264.0 K. [d] K_{eq} = [minor isomer]/[major isomer].

analysis of the variable pressure rate constants for **3** and **4** (Table 5) using eq 4 led to the kinetic parameters summarized in Table 2. Finally, for **3** and **4** the intermolecular exchange with free Me_2SO in the noncoordinating diluent CD_3NO_2 showed that for both dimethyl sulfoxide compounds the exchange rate constant was independent of the concentration of free Me_2SO, consistent with an overall first-order rate law.

(iii) Thermodynamic Measurements on $[(\eta^5\text{-}C_5Me_5)Ir(Me_2SO)_3](PF_6)_2$ (4). The thermodynamic parameters associated with the intramolecular interconversion between the two stereoisomers of **4** were also determined by ^1H NMR spectroscopy. Firstly, measuring the relative changes in population of the bound Me_2SO resonances (i.e., K_{eq}) with temperature (243.2−264.8 K) in the slow-exchange region (Table 4) provided values for $\Delta H°$ and $\Delta S°$ of 15.9 ± 0.5 kJ mol^{-1} and $+50.8 \pm 1.8$ J mol^{-1} K^{-1}, respectively. Secondly, the relative changes in population of the η^5-C_5Me_5 resonances with pressure were also determined (Table 5). A least-squares fit of the pressure data using eq 8 resulted in a value for the volume of reaction accompanying the intramolecular isomerization process, $\Delta V_{intra}°$, of $+9.9 \pm 0.7$ cm^3 mol^{-1}.

$$\ln K_{eq} = \ln K_{eq0} - \Delta V°P/RT \qquad (8)$$

Discussion

(i) Coordination and Conformational Preference. Acetonitrile binds to metal centers solely through its nitrogen atom, as is the case for the two half-sandwich compounds $[(\eta^5\text{-}C_5Me_5)Rh(MeCN)_3](PF_6)_2$ **(1)** and $[(\eta^5\text{-}C_5Me_5)Ir(MeCN)_3](PF_6)_2$ **(2)**, whereas the dimethyl sulfoxide ligand can coordinate to metals *via* oxygen or sulfur.[12] In solution Me_2SO coordinates to rhodium in $[(\eta^5\text{-}C_5Me_5)Rh(Me_2SO)_3](PF_6)_2$ **(3)** by way of the oxygen atom but it instead binds the metal center in $[(\eta^5\text{-}C_5Me_5)Ir(Me_2SO)_3](PF_6)_2$ **(4)** exclusively through the sulfur atom. These bonding assignments were confirmed by Maitlis and co-workers from IR investigations conducted on both Me_2SO and Me_2SO-d_6 analogs of **3** and **4**.[5,13] These assignments are further corroborated by numerous X-ray crystal structures for similar Rh(III) and Ir(III) compounds which illustrate the propensity for the harder rhodium center to bind oxygen and the softer iridium center to coordinate to sulfur.[14] The spectroscopic results we have obtained for **3** and **4** are in complete agreement with these assignments.[15]

Intermolecular solvent exchange on compounds **1**, **2**, and **3** proceeds by a simple exchange process according to eqs 2 and 5, respectively, however; the solvent exchange process is more complex for **4**. Specifically, the intermolecular exchange with free Me_2SO on **4** takes place exclusively from a minor conformer of **4**, depicted as structure **4.2** in Figure 4, which is

(12) Davies, J. A. *Adv. Inorg. Chem. Radiochem.* **1981**, *24*, 115.
(13) Maitlis, P. M. *Acc. Chem. Res.* **1978**, *11*, 301.
(14) (a) Kisenyi, J. M.; Cabeza, J. A.; Smith, A. J.; Adams, H.; Sunley, G. J.; Salt, N. J. S.; Maitlis, P. M. *J. Chem. Soc., Chem. Commun.* **1985**, 770. (b) Sunley, G. J.; Menanteau, P.; Adams, H.; Bailey, N. A.; Maitlis, P. M. *J. Chem. Soc., Dalton Trans.* **1989**, 2415. (c) Krämer, R.; Polborn, K.; Beck, W. *J. Organomet. Chem.* **1991**, *410*, 111. (d) Sokol, V. I.; Rubtsova, N. D.; Gribenyuk, A. Y. *Zh. Strukt. Khim.* **1974**, *15*, 318. (e) Sokol, V. I.; Porai-Koshits, M. A. *Koord. Khim.* **1975**, *1*, 577. (f) Calligaris, M.; Faleschini, P.; Alessio, E. *Acta Crystallogr., Sect. C* **1991**, *47*, 747. (g) Alessio, E; Faleschini, P.; Santi, A. S. O.; Mestroni, G.; Calligaris, M. *Inorg. Chem.* **1993**, *32*, 5756.

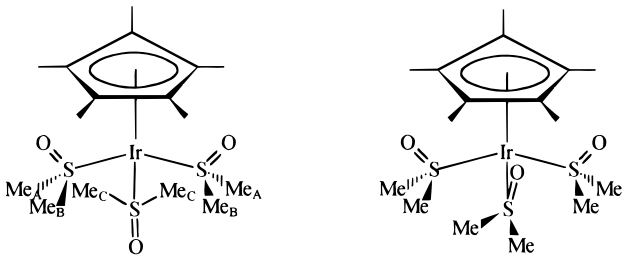

4.1 **4.2**

Figure 4. Structural representations of the major (**4.1**) (two Me_2SO oxygen atoms oriented toward the η^5-C_5Me_5 group, one Me_2SO oxygen atom oriented away) and minor (**4.2**) (all three Me_2SO oxygen atoms oriented toward the η^5-C_5Me_5 group) conformers of $[(\eta^5\text{-}C_5Me_5)Ir(Me_2SO)_3](PF_6)_2$.

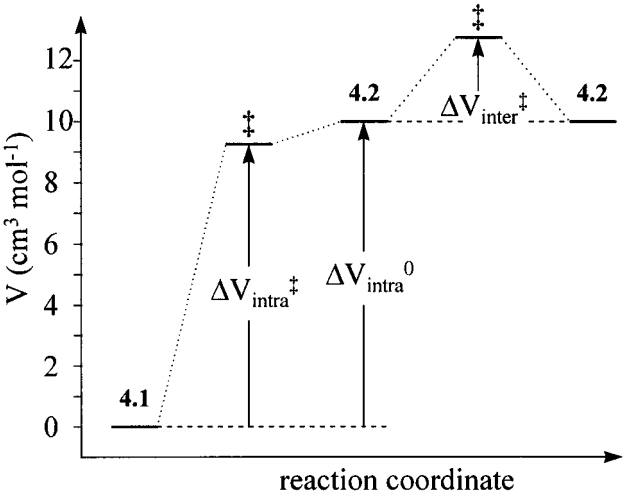

Figure 5. Volume profile for the intramolecular isomerization process and the intermolecular exchange with free Me_2SO on $[(\eta^5\text{-}C_5Me_5)Ir(Me_2SO)_3](PF_6)_2$ **(4)**.

itself in equilibrium with a more compact major conformer of **4** (structure **4.1**; see also eqs 6 and 7).

A detailed description of the solvent exchange process on **4**, including our justification for the assignments of the conformers, is documented in a preliminary communication.[10] We do not repeat the analysis here, but proceed to incorporate the pertinent results into a discussion of the solvent exchange process, focusing on the intramolecular isomerization process on **4** and, most importantly, on the intermolecular exchange with free solvent as observed for all the half-sandwich compounds **1**−**4**.

(ii) Intramolecular Isomerization Process on $[(\eta^5\text{-}C_5Me_5)Ir(Me_2SO)_3](PF_6)_2$ (4). The volume of reaction, ΔV_{intra}°, associated with the isomerization process on **4** (eq 6), from the more populated conformer to the less populated conformer, is +9.9 $cm^3\ mol^{-1}$ (Figure 5). The activation volume, $\Delta V_{intra}^{\ddagger}$, for the same process is slightly smaller than that obtained for the reaction volume. These results infer that the transition state for the interconversion is between **4.1** and **4.2** but more closely resembles the ground state structure **4.2**. Together with the 2D ^1H NMR EXCSY evidence, which established that this isomerization process was intramolecular, the positive value obtained for $\Delta V_{intra}^{\ddagger}$, as defined above, can be ascribed to a lengthening of the M−S bonds in going from structure **4.1** to the sterically crowded structure **4.2** *via* a restricted rotation of the metal−sulfur bond (Figure 4).

A conformational equilibrium was observed for the iridium compound **4** but not for the acetonitrile compounds **1** and **2**, nor for the rhodium dimethyl sulfoxide analog **3**. This is best ascribed to the trigonal-pyrimidal S-bonded Me_2SO ligands in **4** which, within the η^5-C_5Me_5 half-sandwich framework, create a sterically demanding environment which favors specific conformational orientations of these Me_2SO ligands. The steric demands are less for the O-bonded Me_2SO ligands in **3** and insignificant for the linearly bound acetonitrile ligands in **1** and **2**.

(iii) Intermolecular Exchange with Free Solvent. The rate constants and activation parameters for solvent exchange on compounds **1**−**4**, along with their aqua analogs and the corresponding hexaaqua compounds, are summarized in Table 2. The intermolecular exchange with free solvent for the organic solvates of rhodium(III) and iridium(III) is characterized, in each case, by a positive entropy and a positive volume of activation. More importantly, analysis of the solvent exchange in the noncoordinating diluent CD_3NO_2 showed that the exchange rate constant was independent of the concentration of the free solvent for compounds **1**−**4** and, thus, inferred a rate law which was first order. Despite the fact that the activation volumes obtained for these compounds are significantly less positive than those determined for $[Al(Me_2SO)_6]^{3+}$ (+15.6 $cm^3\ mol^{-1}$) and $[Ga(Me_2SO)_6]^{3+}$ (+13.1 $cm^3\ mol^{-1}$), for which a D mechanism was assigned,[16] when they are taken together with the positive entropies of activation and the unambiguous first-order rate laws we can conclude that the solvent exchange process on **1**−**4** is best described by a dissociative D mechanism. Clearly, the volume of activation has been shown to be a powerful tool for the assignment of substitution reaction mechanisms.[16] For the reactions studied in this article the apparent contradiction between the small positive $\Delta V^{\ddagger}$ values and the possibility of a D mechanism may be related to a peculiarity associated with the low-spin t_{2g}^6 electronic configuration of these second- and third-row metal compounds. Further experimental work and theoretical investigations are necessary to better understand these systems.

A previous kinetic study from our laboratory examined the water exchange process on the half-sandwich aqua compounds $[(\eta^5\text{-}C_5Me_5)M(H_2O)_3]^{2+}$ (where M = Rh or Ir).[4] Because of the intrinsic difficulties associated with finding an inert diluent for these aqueous compounds, we were unable to determine a rate law for this system and thus used the evidence at hand (i.e., small well-defined positive activation volumes and less accurate positive entropies of activation) to assign an interchange I mechanism. However, given that the entropies and volumes of activation obtained for the organic solvates **1**−**4** (systems where an unambiguous first-order rate law was determined) are similar to those determined previously for the related half-sandwich aqua compounds, we now suggest that a dissociative pathway is also the operative mechanism for solvent exchange on the η^5-C_5Me_5 aqua compounds.

For the half-sandwich compounds of rhodium, the rates of solvent exchange follow the order of the coligands H_2O > Me_2SO > MeCN (Figure 6). These results suggest that increasing the π-acceptor ability of the bound solvent ligand creates a stronger metal−ligand bond and thus decreases the rate of this dissociatively activated solvent exchange. These effects are also clearly demonstrated by the ruthenium(II)

(15) Spectroscopic data for **4**: (i) ^1H NMR chemical shifts for the coordinated Me_2SO ligands are situated in a region diagnostic of an S-bonded coordination mode; (ii) the close proximity of the chemical shifts corresponding to the major isomer **4.1** is conclusive evidence that all of the Me_2SO ligands are S-bonded; and (iii) at 243.5 K (slow-exchange region) an NOE effect was observed between the methyl substituents of the η^5-C_5Me_5 group and only one of the three ^1H NMR resonances assigned to the major isomer of **4**, corroborating conformer **4.1**.

(16) Merbach, A. E. *Pure Appl. Chem.* **1982**, *54*, 1479.

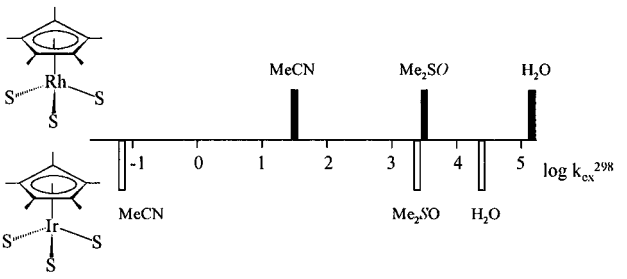

Figure 6. Schematic diagram showing the relative rates of intermolecular exchange with free solvent for compounds **1**−**4** and the corresponding aqua analogs.

compounds $[Ru(H_2O)_6]^{2+}$ and $[Ru(MeCN)_6]^{2+}$, whose rate constants for solvent exchange were measured to be 1.8×10^{-2} and 8.9×10^{-11}, respectively;[17] to the best of our knowledge no quantitative kinetic data is available for solvent exchange on $[Ru(Me_2SO)_6]^{2+}$. Notably, the greater donor strength of Me_2SO compared to H_2O translates into a stronger metal−ligand bond and thus a slower rate of exchange for the dimethyl sulfoxide group in the above series (Figure 6). A similar overall kinetic trend was observed for the iridium half-sandwich compounds; however, the solvent exchange rate constant for the iridium dimethyl sulfoxide compound **4** was faster than expected simply on the basis of our electronic arguments, especially if one considers that the S-bonded Me_2SO ligand in **4** is a better π-acceptor than the O-bonded Me_2SO ligand in **3**.[12] We attribute this unexpectedly large rate constant for **4** to the increased steric crowding around the metal center in this compound, which promotes the dissociation process and thus leads to an increase in the rate of solvent exchange (see also Figure 5).

The rate constant for the iridium acetonitrile species **2** was determined to be *ca.* 3 orders of magnitude smaller than that of its rhodium analog **1** (Figure 6). Since the steric demands in these compounds are minimized by the linearly bound MeCN groups, we can conclude that the difference in the rate constant is due to the larger electronic population on Ir(III), which leads to an increase in the π-back-bonding to the MeCN ligands and, in turn, to a strengthening of the metal−nitrogen bond; the end result is a slower rate of solvent exchange. Consequently, such π-back-bonding does not exist for the H_2O ligands and, as a result, a smaller difference in the rate constants (<1 order of magnitude) was observed for the corresponding η^5-C_5Me_5 aqua compounds of rhodium and iridium.

It is evident that changing the steric and electronic properties of the ligands in the half-sandwich compounds **1**−**4** has a significant effect on the respective rates of solvent exchange, but no apparent effect on the mechanism associated with this process. However, substitution of three bound water molecules in the parent hexaaqua compounds (i.e., $[Rh(H_2O)_6]^{3+}$ or $[Ir(H_2O)_6]^{3+}$) by a η^5-C_5Me_5 moiety resulted in both a large increase in the respective water exchange rate constants (*ca.* 14 orders of magnitude) and a changeover in mechanism from an associative to a dissociative mode of activation. Similar kinetic behavior was reported for the acetonitrile ruthenium(II) couple $[Ru(MeCN)_6]^{2+}/[(\eta^5\text{-}C_5H_5)Ru(MeCN)_3]^{+}$.[17,18] The rate constant for acetonitrile exchange on this system increased by approximately 10 orders of magnitude for the latter compound, and this increase was shown to correlate with a lengthening of the Ru−N bond. On the basis of the work we have presented for the solvento compounds **1**−**4**, we can conclude that these dramatic kinetic changes in both the mechanism and the rate constant are most plausibly ascribed to the electronic and *not* the steric properties of the η^5-C_5Me_5 ligand. That is, the strong electron-donating capability of the η^5-C_5Me_5 group is responsible for strengthening the bond between it and the metal center while concomitantly weakening the remaining three metal−water bonds which occupy positions "trans" to the η^5-C_5Me_5 moiety. Thus, the ligated water molecules become more labile, which, in turn, gives rise to an increase in the rate constant and also favors a dissociative activation process. No such kinetic driving forces are present in the corresponding hexaaqua compounds.

Conclusion

In this paper we have demonstrated that the intermolecular exchange with free solvent on the organic solvates $[(\eta^5\text{-}C_5Me_5)M(S)_3]^{2+}$ (M = Rh, S = MeCN **(1)** or Me_2SO **(3)**; and M = Ir, S = MeCN **(2)** or Me_2SO **(4)**) proceeds, in all cases, *via* a dissociative mechanism. Furthermore, given that the kinetic parameters obtained for the organic solvates **1**−**4** are similar to those determined from previous work on the related aqua compounds $[(\eta^5\text{-}C_5Me_5)M(H_2O)_3]^{2+}$ (M = Rh or Ir),[4] it was suggested that the intermolecular solvent exchange on the latter system also follows a dissociative pathway. With respect to the parent hexaaqua compounds, the rate constants associated with the solvent exchange process on the half-sandwich species were shown to be governed primarily by the electronic properties of the ligands; clearly the strong electron-donating capability of the η^5-C_5Me_5 group and the π-acceptor capability of the other coligands are the two most important properties.

Acknowledgment. We thank the Swiss National Science Foundation for financial support.

Supporting Information Available: Observed first-order rate constants as a function of free MeCN concentration for MeCN exchange on $[(\eta^5\text{-}C_5Me_5)Rh(MeCN)_3](PF_6)_2$ **(1)** (Table S1), observed first-order rate constants as a function of free Me_2SO concentration (Table S3) and a plot of chemical shift vs temperature (Figure S1) for Me_2SO exchange on $[(\eta^5\text{-}C_5Me_5)Rh(Me_2SO)_3](PF_6)_2$ **(3)**, Kubo−Sack matrix elements (Table S2), observed first-order rate constants as a function of free Me_2SO concentration (Table S4) and a plot of chemical shift vs temperature (Figure S2) for Me_2SO exchange on $[(\eta^5\text{-}C_5Me_5)Ir(Me_2SO)_3](PF_6)_2$ **(4)**, and experimental ^1H NMR (400 MHz) spectra of $[(\eta^5\text{-}C_5Me_5)Rh(Me_2SO)_3](PF_6)_2$ **(3)** (0.100 m) in CD_3NO_2 diluent ([free Me_2SO] = 0.304 m) acquired using the high pressure probe at 276.0 K illustrating the effect of pressure on the Me_2SO exchange rate and the resolution on TMS (Figure S3) (7 pages). Ordering information is given on any current masthead page.

IC961380L

(17) (a) Rapaport, I.; Helm, L.; Merbach, A. E.; Bernhard, P.; Ludi, A. *Inorg. Chem.* **1988**, *27*, 873. (b) Davies, A. R.; Einstein, F. W. B.; Farrell, N. P.; James, B. R.; McMillan, R. S. *Inorg. Chem.* **1978**, *17*, 1965. (c) Aebischer, N.; Laurenczy, G.; Ludi, A.; Merbach, A. E. *Inorg. Chem.* **1993**, *32*, 2810.

(18) Luginbühl, W.; Zbinden, P.; Pittet, P. A.; Armbruster, T.; Bürgi, H.-B.; Merbach, A. E.; Ludi, A. *Inorg. Chem.* **1991**, *30*, 2350.